Charge transfer based "turn-on" chemosensor for Zn^{2+} ion recognition using new triaryl pyrazoline derivative

Dharmaraj Jeyanthi, Murugan Iniya, Karuppiah Krishnaveni, Duraisamy Chellappa

PII: S1386-1425(16)30027-0
DOI: doi: 10.1016/j.saa.2016.01.027
Reference: SAA 14237

To appear in:

Received date: 19 July 2015
Revised date: 12 January 2016
Accepted date: 19 January 2016

Please cite this article as: Dharmaraj Jeyanthi, Murugan Iniya, Karuppiah Krishnaveni, Duraisamy Chellappa, Charge transfer based "turn-on" chemosensor for Zn^{2+} ion recognition using new triaryl pyrazoline derivative, (2016), doi: 10.1016/j.saa.2016.01.027

Charge transfer based "turn-on" Chemosensor for Zn^{2+} ion recognition using new Triarylpyrazoline derivative

Dharmaraj Jeyanthi [a], Murugan Iniya [a], Karuppiah Krishnaveni [a] and Duraisamy Chellappa*[a]

[a]School of Chemistry, Madurai Kamaraj University, Madurai, TamilNadu-625021, India.

**Corresponding author. Tel: +91 452 2456614; Fax: +91 452 2459181.*

E-mail address: dcmku123@gmail.com

Abstract

The fluoroionophore **PY** serves as a selective and fluorimetric chemosensor for Zn^{2+} based on charge transfer(CT). A mechanism for the binding mode was proposed based on fluorescence changes, NMR experiments and theoretical calculations. The 1:1 stoichiometry between Zn^{2+} and the sensor was deduced from Job's plot. The addition of EDTA quenches the fluorescence of **PY.Zn^{2+}** complex offers **PY** as a reversible chemosensor.

Keywords: charge transfer; triaryl pyrazoline; fluorimetric changes; reversibility

1. Introduction

Fluorescent chemosensors for metal ions are indispensable tool and have received extensive attention in light of their diverse applications in areas like environment, biology, chemistry and medicine [1,2]. Zinc, the second most abundant and essential trace divalent transition-metal after iron in the living systems, is an essential cofactor of many biological processes such as catalytic centers, regulators of gene expressions and enzymes[3-5]. Zinc is also a contributory factor in several neurodegenerative diseases exemplified as epilepsy, ischemia, stroke, Alzheimer's and Parkinson's diseases [6].

Moreover, apart from its wide applications, a high level of zinc is highly toxic and leads to diabetes, skin disease and prostatic adeno carcinoma [7] and reduce the soil microbial activity causing phytotoxic effects [8,9]. For Zn^{2+} sensing, fluorescence techniques are used because of their high sensitivity, accurate determination and spatiotemporal resolution than other detection methods [10, 11]. Thus development of simple, selective and accessible fluorescent sensors for Zn^{2+} is crucially important and strongly required for environmental and biological analysis [12].

The fluorescent activities of sensor was controlled by a number of mechanisms such as Charge transfer transitions(CT)[13], Photo electron transfer(PET)[14,15], Chelation enhanced fluorescence(CHEF)[16], Fluorescence resonance energy transfer(FRET)[17], and Excimer formation[18]. Pyrazoline derivatives have many interesting bioactivities such as antimicrobial [19], antiamoebic[20], anticancer[21], antinociceptive[22], antidepressant[23] and anti-inflammatory[24]. Up to now, only few fluorescent reports based on this class of compounds are available for Zn^{2+} detection compared to other heavy metal ions [25-30].

In continuation of our on-going research in the development of metal ion sensors [31-33], herein we have designed a relatively simple triaryl pyrazole derivative as a metal chelating moiety. It has selective binding affinity towards Zn^{2+} and exhibits sensitive "turn-on" fluorescence operating through charge transfer mechanism.

2. Experimental Section

2.1. Materials and methods

All the chemicals were purchased from Sigma-Aldrich and used as received unless otherwise mentioned. Metal chloride salts obtained from Sigma-Aldrich were used as sources for metal ions. Solvents used

were of spectroscopic grade. UV-visible absorption spectra were recorded on JASCO V-550 spectrometer. All fluorescence measurements were made on an F-4500 Hitachi fluorescence spectrophotometer with slit width 5nm used for both excitation and emission. The NMR spectra were recorded on a Bruker (Avance) instrument operating at 300MHz in DMSO-d_6 with tetramethylsilane as an internal reference. Chemical shifts were expressed in ppm and coupling constants(J) in Hz. Electrospray ionization mass spectrometry (ESI-MS) analysis was performed in the positive ion mode on a liquid chromatography-ion trap mass spectrometer(LCQ fleet, Thermo Fisher Instruments Limited, US). Elemental analysis was carried out in a Perkin-Elmer 4100 elemental analyzer. The stock solution of the probe (10μM) was prepared in DMSO. The solutions of metal ions were prepared from their chloride salts. Metal ion stock solutions were prepared in deionized water keeping concentration range from 0-10μM. Doubly distilled deionized water was used throughout. All titrations were carried out at room temperature. For the fluorescence spectra, the excitation wavelength was kept at 350nm.

2.2. General synthetic procedure for the preparation of (5-(4-chlorophenyl)-3-(4-hydroxyphenyl)-1H-pyrazol-1-yl)(2-hydroxyphenyl)methanone(PY)

Starting materials chalcone and 2-hydroxybenzohydrazide were prepared according to literatures. To a stirred solution of chalcone (0.500g, 1.0mmol) in ethanol was added 2-hydroxybenzohydrazide (0.353g, 1.2mmol) and NaOH (0.233g, 3.0mmol). The reaction mixture was refluxed for 4h. The progress of the reaction was monitored by TLC. After completion, the reaction mixture was cooled to room temperature and diluted with chilled water, and then hydrochloric acid was added to neutralize it. The crude product was obtained as yellow precipitates. The precipitate was filtered, washed with water and ethanol and then subsequently recrystallized from ethanol to afford product (PY). ^{1}H NMR(300MHz, DMSO-d_6, TMS): δ(ppm) = 11.20(s, 1H, OH), 10.50(s, 1H, OH), 8.66(s, 1H, pyrazole-1H), 8.06(d, 1H, J=8.7Hz, Ar-H), 6.87-7.95(m, 12H, Ar-H). ^{13}C NMR(75MHz, DMSO d_6, TMS): δ(ppm)=187.35, 162.62, 141.40, 135.01, 134.14, 131.44, 130.54, 129.29, 129.13, 123.28, 115.7. IR (KBr, cm^{-1}): ν(O-H), 3452; ν(C-H), 3050; ν(C=O), 1706; ν(C=N), 1650; ν(M-O), 628;ν(M-N), 528. Anal. Calcd for $C_{12}H_{15}ClN_2O_3$: C 67.61, H 3.87,Cl 9.07, N 7.17, O 12.28; Found: C 68.0, H 3.85, Cl 8.80, N 7.13, O 12.22%; MS (ESI): 391$(M+H)^+$.

2.3. Computational details

Density functional theory (DFT) calculations were carried out with B3LYP-6-31G and B3LYP/LanL2DZ basis set using Gaussian 03 program package to confirm the UV-visible and

fluorescence changes upon the addition of Zn^{2+} ion. The TD-DFT calculations on the optimized geometries of **PY** & **PY.Zn^{2+}** were performed using the above basis set in order to obtain the electronic behavior and oscillator strength for the electronic transitions.

3. Results and discussion

Scheme 1

The receptor was synthesized by a simple and straightforward method with good yield by condensation of chalcone with salicyloyl hydrazide in methanol as depicted in **scheme 1**. The receptor was systematically and fully characterized by ^{1}H, ^{13}C-NMR, FT-IR, ESI-MS and elemental analysis (**Fig S1-S5, ESI†**). To explore the practical utility of the probe in bio-environment, the signal response of probe **PY** upon subjecting to interaction with different metal ions was monitored using both absorption and emission spectrometers in aqueous DMSO [DMSO: H_2O=8:2] at pH=7.4 (HEPES buffer). The uv-vis spectral response of **PY** (10μM) towards Zn^{2+} and other metal ions are given in **Fig. 1.**

Fig. 1

It is obvious from the spectra that only Zn^{2+} ion induced an observable change in the absorption spectrum of probe **PY**. However, other metal ions cause least variation in the absorption spectra (**Fig. 1**). The absorption intensity at 308nm decreased linearly with increasing concentration of Zn^{2+} (0-10μM). Simultaneously a new absorption peak appeared and gradually increased at 372nm upon addition of Zn^{2+} ion with distinct isobestic point at 350nm. The new peak at 372nm increased up to the addition of 1equivalent of Zn^{2+} and leveled off thereafter, indicating a molar ratio (**PY**/Zn^{2+}) of 1:1 (**Fig. S6**). This observation in absorption spectra is attributable to an interaction between Zn^{2+} and the receptor **PY** in ground state.

Fig. 2

To gain further insight into the sensing properties and mechanism, emission profile of sensor molecule **PY** upon interaction with different metal ions were examined (**Fig. S7**). Only Zn^{2+} induced sizable enhancement in the fluorescence spectra of **PY**[34]. Negligible change in emission spectra was observed for other tested metal ions such as Na^{+}, K^{+}, Li^{+}, Ag^{+}, Ca^{2+}, Mg^{2+}, Cu^{2+}, Co^{2+}, Ni^{2+}, Mn^{2+}, Zn^{2+},

Cd^{2+}, Hg^{2+}, Pb^{2+},Cr^{3+}, Al^{3+}, Fe^{3+} even when present in excess (**Fig. S8**). The fluorescence titration of ligand PY was performed with increasing concentration of Zn^{2+} (0-10μM) in DMSO/H_2O system [DMSO: H_2O=8:2] at pH = 7.4 (HEPES buffer).

Fig. 3

Fig. 4

PY shows a weak fluorescent emission band at 446nm when excited at 350nm (φ_f=0.03). Upon sequential addition of Zn^{2+} the emission band at 446nm undergoes a red shift by 12nm with hyperchromism to 458nm (quantum yield φ_f=0.31) (ESI†) at room temperature (**Fig. 2**). The emission intensity reached maximum when the amount of Zn^{2+} reached 1equivalent thereby suggests 1:1 stoichiometry between **PY** and Zn^{2+}. This was further confirmed by Job's plot. The fluorogenic changes of **PY** with Zn^{2+} is shown in **Fig. 3**. The observed dramatic red shift in the fluorescence emission could be a result of charge transfer mechanism (CT). A proposed binding mode is given in **Fig. 4**

Fig. 5

In order to determine the stoichiometry of complex formed between **PY** and Zn^{2+}, the method of continous variation (Job's method)[35,36] using the emission changes was applied by varying the mole fraction of Zn^{2+} from 0.1 to 0.9 and by keeping the sum of the concentration of Zn^{2+} and **PY** as constant (**Fig. 5**). The emission maximum was observed when the mole fraction of Zn^{2+} reached 0.5, in accordance with the proposed host-guest binding stoichiometry.

Fig. 6

The composition of complex **PY.Zn^{2+}** (1:1) has also been proved by ESI-MS analysis. The receptor **PY** shows m/z at 391 corresponding to $[M+H]^+$ ion, where M = PY; for **PY.Zn^{2+}** complex the observed m/z peak at 514 corresponding to $[M-H+Na]^+$, where M=$[PY+Zn^{2+}+Cl^-]$, confirms 1:1 binding stoichiometry. From the fluorescence titration profile of **PY** with Zn^{2+}, the association constant ka was found to be $2.4x10^4M^{-1}$(ESI†) (**Fig. 6**)[37]. In addition, the detection limit of **PY** for the analysis of Zn^{2+} was calculated to be 1.02μM (ESI†); this shows that **PY** is a more effective and excellent fluorescent sensor for Zn^{2+} over other cations[38]. The calculated association constant and detection limit are tabulated with that reported in the literature respectively in (Table 1) and (Table 2). On comparison it is clear that the present probe resembles many of the reported probes in its binding constant. Also obvious is

that the present probe is having higher efficiency in detection of zinc relative to benzimidazole based receptor but lower efficiency with reference to probes like MCB dye.

Fig. 7

To check out the potential utility and efficiency of **PY** for Zn^{2+}, the competitive experiments were conducted in the presence of other biologically relevant cations under the same conditions (**Fig. 7**). The results showed insignificant effect on Zn^{2+}-induced fluorescence enhancement. Thus, this probe should have good selectivity and remarkable sensitivity for Zn^{2+} in the biological studies. To gain further insight into the reversible behavior of the receptor PY towards Zn^{2+}, the effect of addition of chelator EDTA was examined (**Fig. S9**). This feature is highly desirable for practical applications and to rule out the possibility that the fluorescent enhancement observed is not due to a chemical reaction [(i.e) chemodosimeter][39]. It revealed that addition of 1 equivalent of EDTA to the **PY.Zn^{2+}** complex results in recovery of original fluorescence spectra of **PY**. The same extent of fluorescence enhancement was again recovered by the addition of another 1equivalent of free Zn^{2+} ions. It shows the reversible nature of binding interaction between **PY** and Zn^{2+}.

Fig. 8

To get insight into cation binding interaction of **PY** with Zn^{2+}, ^{1}H NMR titrations were also carried out in d_6-DMSO at room temperature. The changes in the ^{1}H NMR spectra of **PY** before and after the addition of Zn^{2+} (0.5, 1.0equivalent) are shown in **Fig. 8**. All aromatic protons in the receptor **PY**, showed a downfield shift upon chelation to Zn^{2+}. When **PY** interact with 0.5equivalent of Zn^{2+}, the –OH proton of salicyloyl hydrazide moiety underwent downfield shift with broadening and disappeared on addition of 1equivalent Zn^{2+} indicating the involvement of the phenolic oxygen atom in complexing the metal ion via deprotonation. Moreover, Zn^{2+} coordination also triggers a clear downfield shift of the pyrazole protons. All these findings indicated a proposed binding mode of **PY** with Zn^{2+} and the dynamic nature of the zinc sensing process. In addition, almost same fluorescent enhancement of **PY** was noted after the addition of different counter anionic zinc salts such as $Zn(NO_3)_2$, $ZnCl_2$, $ZnSO_4$ and $Zn(OAc)_2$ (**Fig. 9**). The result reveals the influence of counter anions on the detection of Zn^{2+} with **PY** is rather small. In otherwords, the anion effect of different zinc salts is insignificant.

Fig. 9

Fig. 10

3.1. DFT Calculations

The bathochromic shift of the emission of probe upon binding with Zn^{2+} and plausible reason for that was elucidated using quantum calculations. The geometries of receptor **PY** and **PY.Zn^{2+}** optimized in the ground state using density functional theory (DFT) with Becke's three parameter hybrid exchange functional (B3LYP) but using basis set 6-31G(d,p) and LANL2D(d) levels respectively, are shown in **Fig. 10**. To further gauge the electronic behavior of the probe in the presence and absence of Zn^{2+}, time dependent density functional theory (TD-DFT) calculations were carried out using the same functional and basis set. All above computations were performed with Gaussian 03 program package [40].

Fig. 11

The zinc is bound by one N-atom (not adjacent to >C=O group) from pyrazole ring, carbonyl oxygen, phenolic oxygen and one chloride ion in a distorted tetrahedral arrangement. **Fig. 11** shows calculated HOMO and LUMO of **PY** and **PY.Zn^{2+}**. In **PY** HOMO resides on molecule bearing chlorophenyl moiety while LUMO spans only pyrazole and salicyloyl moieties. In **PY.Zn^{2+}**, HOMO almost resembles that of pure probe **PY**, while LUMO resides intensively on Zn^{2+} ion. This indicates substantial charge transfer from donor moiety to Zn^{2+} when the molecule is excited. Furthermore, the lowering of HOMO-LUMO energy gap after Zn^{2+} binding corroborates the experimentally observed red shift of emission band [41] (**Fig. S10**). Therefore, based on the above analysis, the proposed mechanism is rational and reasonable.

4. Conclusion

In conclusion, we have designed and successfully synthesized a new triaryl pyrazole derivative (**PY**) as a good selective and sensitive "turn-on" fluorescent sensor for Zn^{2+} over other cations. The structure was confirmed by ^{1}H, ^{13}C-NMR, mass spectrometric and elemental analysis. Based on DFT/TD-DFT calculations it is proposed that ligand to metal charge transfer is responsible for fluorescence enhancement. These findings clearly demonstrate that **PY** could be applied as a strong sensor for Zn^{2+} with biological applications.

Acknowledgement

The authors D.J., M.I., K.K., are grateful to UGC-BSR for research fellowship and also thankful to DST-IRHPA, FIST and PURSE for funding and instrumental facilities.

References

1. A.P. De Silva, H.Q.N. Gunaratne, T. Gunlaugsson, A.J.M. Huxley, C.P. McCoy, J.T. Rademacher, T.E. Rice, Chem. Rev., 97 (1997) 1515-1566.
2. J.F. Callan, A.P. de Silva, D.C. Magri, Tetrahedron, 61 (2005) 8551-8588.
3. (a) J.M. Berg, Y. Shi, Science, 271 (1996) 1081-1085; (b) M. Lu, D. Fu, Science, 317 (2007) 1746-1748; (c) D.H. Nies, Science, 317 (2007) 1695-1696.
4. S.C. Burdette, S.J. Lippard, Proc. Natl. Acad. Sci. U. S. A., 100 (2003) 3605-3610.
5. J.J.R.F. de Silva, R.J.P. Williams, The Biological Chemistry of Elements: The Inorganic Chemistry of Life, second ed., Oxford University Press, New York, 2001.
6. (a) A. Helal, H.S. Kim, Tetrahedron Lett., 50 (2009) 5510-5515; (b) J.H. Weiss, S.L. Sensi, J.Y. Koh, Trends. Pharmacol. Sci., 21 (2000) 395-401.
7. (a) A. Azam, H.M. Chawla, S. Pandey, Tetrahedron Lett., 51 (2010) 4710-4711; (b) S.H. Mashraqui, T. Khan, S. Sundaram, R. Betkar, M. Chandiramani, Tetrahedron Lett., 48 (2007) 8487-8490.
8. A. Voegelin, S. Pfister, A.C. Scheinost, M.A. Marcus, R. Kretzschmar, Environ. Sci. Technol., 39 (2005) 6616-6623.
9. E. Callender, K.C. Rice, Environ. Sci. Technol., 34 (2000) 232-238.
10. Z. Xu, J. Yoon, D.R. Spring, Chem. Soc. Rev., 39 (2010) 1996-2006.
11. E. Tomat, S.J. Lippard, Curr. Opin. Chem. Biol., 14 (2010) 225-230.
12. (a) D. Buccella, J.A. Horowitz, S.J. Lippard, J. Am. Chem. Soc., 133 (2011) 4101-4114; (b) S.K. Rastogi, P. Pal, D.E. Aston, T.E. Bitterwolf, A.L. Branen, ACS Appl. Mater. Interfaces, 3 (2011) 1731-1739; (c) A. Krezel, J. Wojcik, M. Maciejczyk, W. Bal, Inorg. Chem., 50 (2011) 72-85; (d) E. Tomat, S.J. Lippard, Inorg. Chem., 49 (2010) 9113-9115; (e) S.Y. Kim, J.I. Hong, Tetrahedron Lett., 50 (2009) 2822-2824; (f) L. Xue, H.H. Wang, H. Jiang, Inorg. Chem., 47 (2008) 4310-4318; (g) C.C. Woodroofe, A.C. Won, S.J. Lippard, Inorg. Chem., 44 (2005) 3112-3120.
13. F. Qian, C.L. Zhang, Y.M. Zhang, W.J. He, X. Gao, P. Hu, Z.J. Guo, J. Am. Chem. Soc., 131 (2009) 1460-1468.
14. L. Xue, C. Liu, H. Jiang, Org. Lett., 11 (2009) 1655-1658.

15. S. Lzumi, Y. Urano, K. Hanaoka, T. Terai, T. Nagano, J. Am. Chem. Soc., 131 (2009) 10189-10200.
16. N.C. Lim, J.V. Schuster, M.C. Porto, M.A. Tanudra, L. Yao, H.C. Freake, Inorg. Chem., 44 (2005) 2018-2030.
17. S.Y. Lee, H.J. Kim, J.S. Wu, K. No, J.S. Kim, Tetrahedron Lett., 49 (2008) 6141-6144.
18. (a) S.K. Kim, D.H. Lee, J.I. Hong, J. Yoon, Acc. Chem. Res., 42 (2009) 23-31; (b) S.W. Thomas. G.D. Joly, T.M. Swager, Chem. Rev., 107 (2007) 1339-1386.
19. K. Manna, Y.K. Agrawal, Bioorg. Med. Chem. Lett., 19 (2009) 2688-2692.
20. A. Budakoti, A.R. Bhat, A. Azam, Eur. J. Med. Chem., 44 (2009) 1317-1325.
21. D. Havrylyuk, B. Zimenkovsky, O. Vasylenko, L. Zaprutko, R. Lesyk, Eur. J. Med. Chem., 2009, 44, 1396-1404.
22. Z.A. Kaplancikli, G. Turan-Zitouni, A. Ozdemir, O.D. Can, P. Chevallet, Eur. J. Med. Chem., 44 (2009) 2606-2610.
23. N. Gokhan-Kelekci, S. Koyunoglu, S. Yabanoglu, Bioorg. Med. Chem., 17 (2009) 675-689.
24. I.G. Rathish, K. Javed, S. Ahmad, S. Bano, Bioorg. Med. Chem. Lett., 19 (2009) 255-258.
25. S.M. Song, D. Ju, J. Li, D. Li, Y. Wei, C. Dong, P. Lin, S. Shuang, Talanta, 77 (2009) 1707-1714.
26. Z. Xu, K.H. Baek, H.N. Kim, J. Cui, X. Qian, D.R. Spring, I. Shin, J. Yoon, J. Am. Chem. Soc., 132 (2010) 601-610.
27. J.Y. Choi, D. Kim, J. Yoon, Dyes Pigm., 98 (2013) 176-179.
28. Z. Guo, G.H. Kim, I. Shin, J. Yoon, Biomaterials, 33 (2012) 7818-7827.
29. T.T. Zhang, X.P. Chen, J.T. Liu, L.Z. Zhang, J.M. Chu, L. Su, B.X. Zhao, RSC Adv., 4 (2014) 16973-16978.
30. G. Zhang, H. Li, S. Bi, L. Song, Y. Lu, L. Zhang, J. Yu, L. Wang, Analyst, 138 (2013) 6163-6170.
31. D. Jeyanthi, M. Iniya, K. Krishnaveni, D. Chellappa, RSC Adv., 3 (2013) 20984-20989.
32. M. Iniya, D. Jeyanthi, K. Krishnaveni, A. Mahesh, D. Chellappa, Spectrochim. Acta A, Mol. Biomol. Spectrosc., 120 (2014) 40-46.
33. M. Iniya, D. Jeyanthi, K. Krishnaveni, D. Chellappa, Rsc. Adv., 4 (2014) 25393-25397.
34. (a) S. Lee, J.H. Lee, T. Pradhan, C.S. Lim, B.R. Cho, S. Bhuniya, S. Kim, J.S. Kim, Sens. Actuators, B. 160 (2011) 1489-1493; (b) J.F. Zhang, S. Kim, J.H. Han, S.J. Lee, T. Pradhan, Q.Y. Cao, S.J. Lee, C. Kang, J.S. Kim, Org. Lett. 13 (2011) 5294-5297.
35. W.C. Vosburgh, G.R. Cooper, J. Am. Chem., Soc., 63 (1941) 437-442.

36. R.R. Avirah, K. Jyothish, D. Ramaiah, Org. Lett., 9 (2007) 121-124.
37. K. A. Conners, Binding Constants, Wiley, New York, 1987.
38. M. Shortreed, R. Kopelman, M. Kuhn, B. Hoyland, Anal. Chem., 68 (1996) 1414-1418.
39. K.C. Song, J.S. Kim, S.M. Park, K.C. Chung, S. Ahn, S.K. Chang, Org. Lett., 8 (2006) 3413-3416.
40. Gaussian 03, Revision C.02, M.J. Frisch, G. Trucks, H.B. Schlegel, G.E. Scuseria, M.A. Robb, J.R. Cheeseman, J.A. Montgomery, T. Vreven, K.N. Kudin, J.C. Burant, J.M. Millam, S.S. Iyengar, J. Tomasi, V. Barone, B. Mennucci, M. Cossi, G. Scalmani, N. Rega, G.A. Petersson, H. Nakatsuji, M. Hada, M. Ehara, K. Toyota, R. Fukuda, J. Hasegawa, M. Ishida, T. Nakajima, Y. Honda, O. Kitao, H. Nakai, M. Klene, X. Li, J.E. Knox, H.P. Hratchian, J.B. Cross, V. Bakken, C. Adamo, J. Jaramillo, R. Gomperts, R.E. Stratmann, O. Yazyev, A.J. Austin, R. Cammi, C. Pomelli, J.W. Ochterski, P.Y. Ayala, K. Morokuma, G.A. Voth, P. Salvador, J.J. Dannenberg, V.G. Zakrzewski, S. Dapprich, A.D. Daniels, M.C. Strain, O. Farkas, D.K. Malick, A.D. Rabuck, K. Raghavachari, J.B. Foresman, J.V. Ortiz, Q. Cui, A.G. Baboul, S. Clifford, J. Cioslowski, B.B. Stefanov, G. Liu, A. Liashenko, P. Piskorz, I. Komaromi, R.L. Martin, D.J. Fox, T. Keith, M.A. AlLaham, C.Y. Peng, A.Nanayakkara, M. Challacombe, P.M.W. Gill, B. Johnson, W. Chen, M.W. Wong, C. Gonzalez, J.A. Pople, Gaussian, Inc., Wallingford CT, 2004.
41. Y.P. Li, H.R. Yang, Q. Zhao, W.C. Song, J. Han, X.H. Bu, Inorg. Chem., 51 (2012) 9642-9648.

Figure Captions

Scheme 1. The synthetic route of receptor PY

Fig 1. UV-vis absorption spectra of PY(10μM) in the presence of various metal ions($1x10^{-5}$M) like Na^{+}, K^{+}, Li^{+}, Ag^{+}, Ca^{2+}, Mg^{2+}, Cu^{2+}, Co^{2+}, Ni^{2+}, Mn^{2+}, Zn^{2+}, Cd^{2+}, Hg^{2+}, Pb^{2+}, Cr^{3+}, Al^{3+}, Fe^{3+} in aqueous DMSO[DMSO:H_2O=8:2] at pH = 7.4 (HEPES buffer).

Fig 2. Changes in fluorescence intensity of PY(10μM) in aqueous DMSO[DMSO:H_2O=8:2] at pH = 7.4 (HEPES buffer) upon successive addition of Zn^{2+}(0-1 equivalent). Excitation wavelength = 350nm

Fig 3. Fluorogenic changes of a 10μM solution of PY in aqueous DMSO[DMSO:H_2O=8:2] at pH = 7.4 (HEPES buffer) in the presence of 1 equivalent Zn^{2+} (irradiated by 365nm light)

Fig 4. A proposed binding mode of PY for Zn^{2+}

Fig 5. Job's plot for the complex formed between receptor PY and Zn^{2+}

Fig 6. Plot of fluorescence intensity variation at 458nm upon varying equivalents of Zn^{2+} ions

Fig 7. The fluorescence intensity of PY(10μM) in the presence of 20μM for Na^{+}, K^{+}, Li^{+}, Ag^{+}, Ca^{2+}, Mg^{2+}, Cu^{2+}, Co^{2+}, Ni^{2+}, Mn^{2+}, Zn^{2+}, Cd^{2+}, Hg^{2+}, Pb^{2+}, Cr^{3+}, Al^{3+}, Fe^{3+} (violet bars) followed by addition of 10μM of Zn^{2+} (pink bars) in aqueous DMSO[DMSO:H_2O=8:2] at pH = 7.4 (HEPES buffer). Excitation at 350nm (slit width=5nm)

Fig 8. Plot of ^{1}H NMR spectra of receptor PY(10μM) upon addition of Zn^{2+} in DMSO-d_6 at room tempertature

Fig 9. Fluorescent emission spectra of free receptor PY($1x10^{-5}$M) in aqueous DMSO[DMSO: H_2O=8:2] at pH = 7.4 (HEPES buffer) upon addition of 1.0 equivalent of different zinc salts

Fig 10. Conformations of PY(left) and PY.Zn^{2+}(right) optimized by density functional theory calculations

Fig 11. HOMO and LUMO plot of PY & PY/Zn^{2+} calculated at B3LYP/LANL2DZ(d) level of theory

Figures

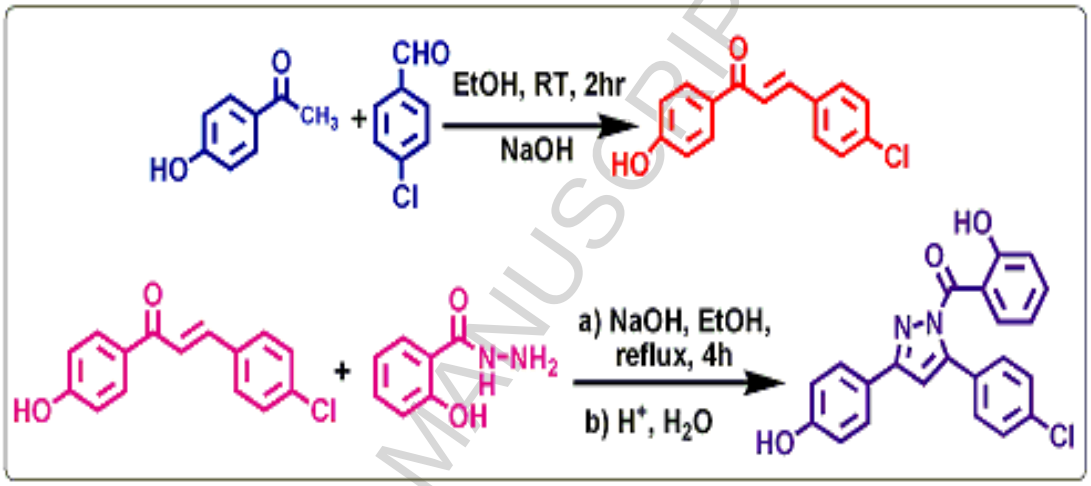

Scheme 1. The synthetic route of receptor PY

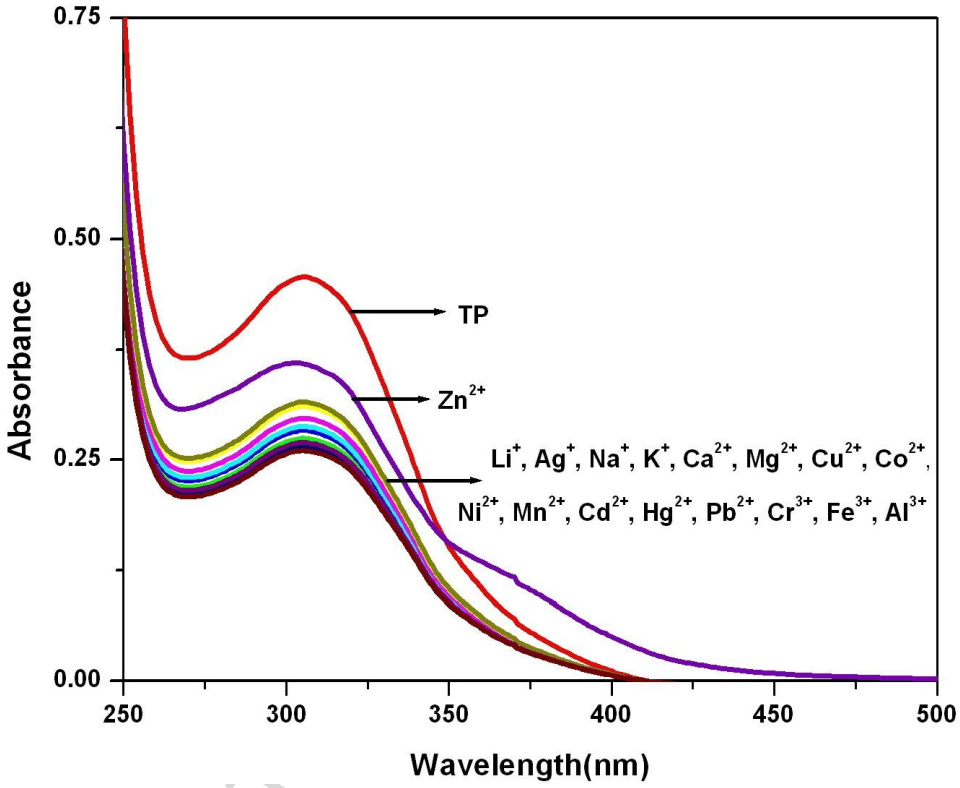

Fig 1. UV-vis absorption spectra of PY(10µM) in the presence of various metal ions($1x10^{-5}$M) like Na^+, K^+, Li^+, Ag^+, Ca^{2+}, Mg^{2+}, Cu^{2+}, Co^{2+}, Ni^{2+}, Mn^{2+}, Zn^{2+}, Cd^{2+}, Hg^{2+}, Pb^{2+}, Cr^{3+}, Al^{3+}, Fe^{3+} in aqueous DMSO[DMSO:H_2O=8:2] at pH = 7.4 (HEPES buffer).

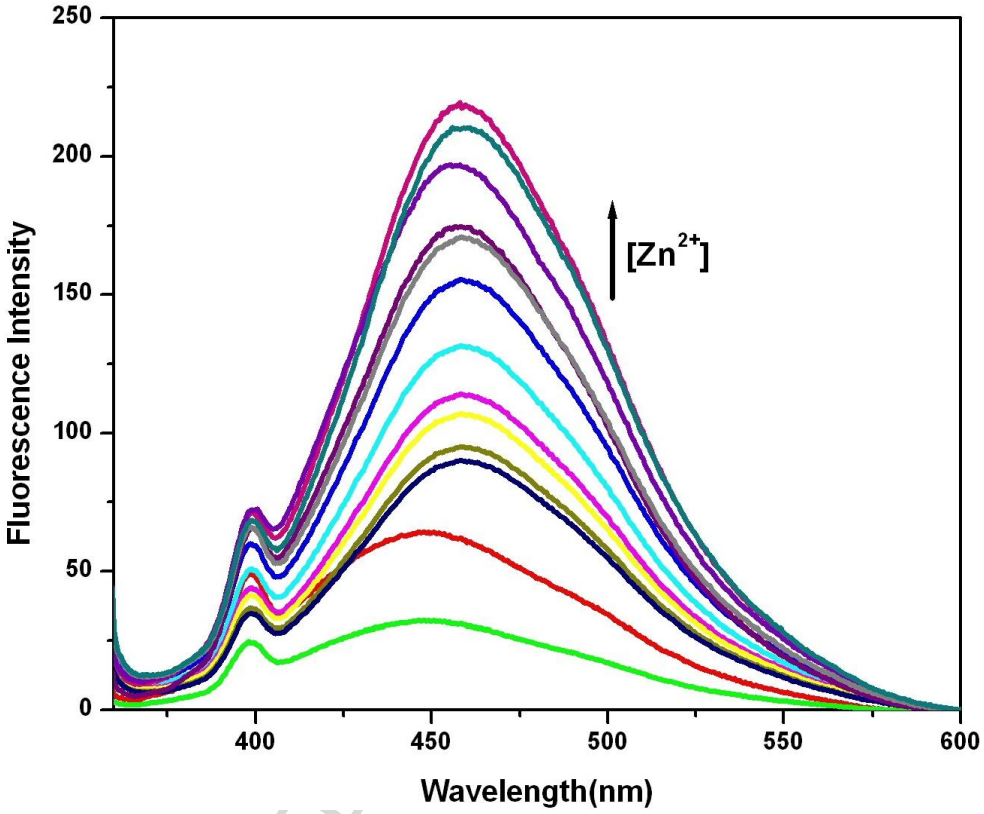

Fig 2. Changes in fluorescence intensity of PY(10μM) in aqueous DMSO[DMSO:H_2O=8:2] at pH = 7.4 (HEPES buffer) upon successive addition of Zn^{2+}(0-1 equivalent). Excitation wavelength = 350nm

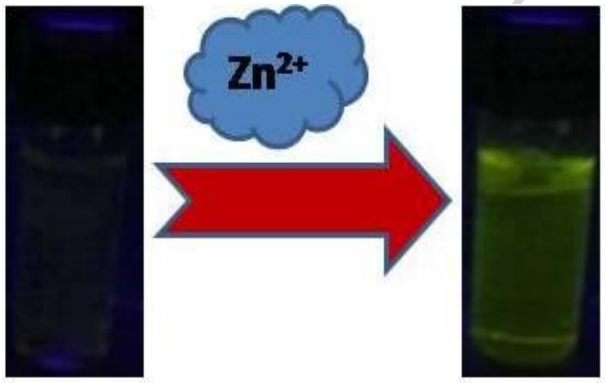

Fig 3. Fluorogenic changes of a 10μM solution of PY in aqueous DMSO[DMSO:H_2O=8:2] at pH = 7.4 (HEPES buffer) in the presence of 1 equivalent Zn^{2+} (irradiated by 365nm light)

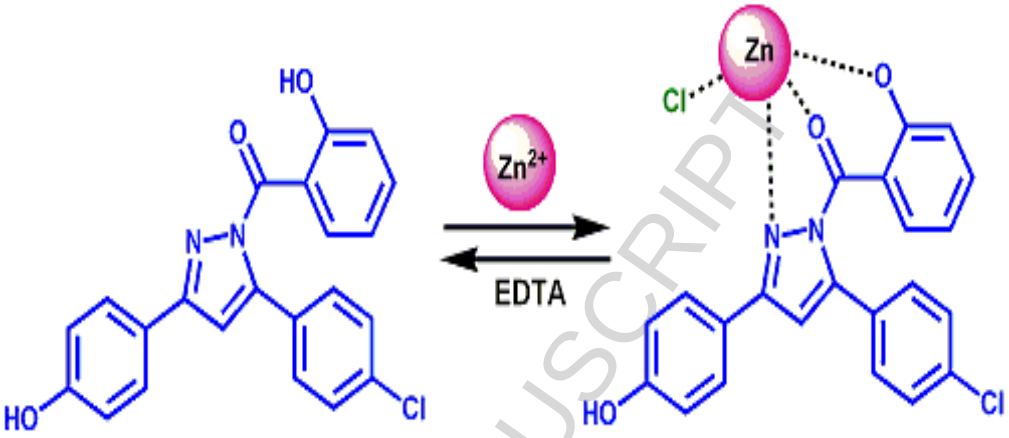

Fig 4. A proposed binding mode of PY for Zn^{2+}

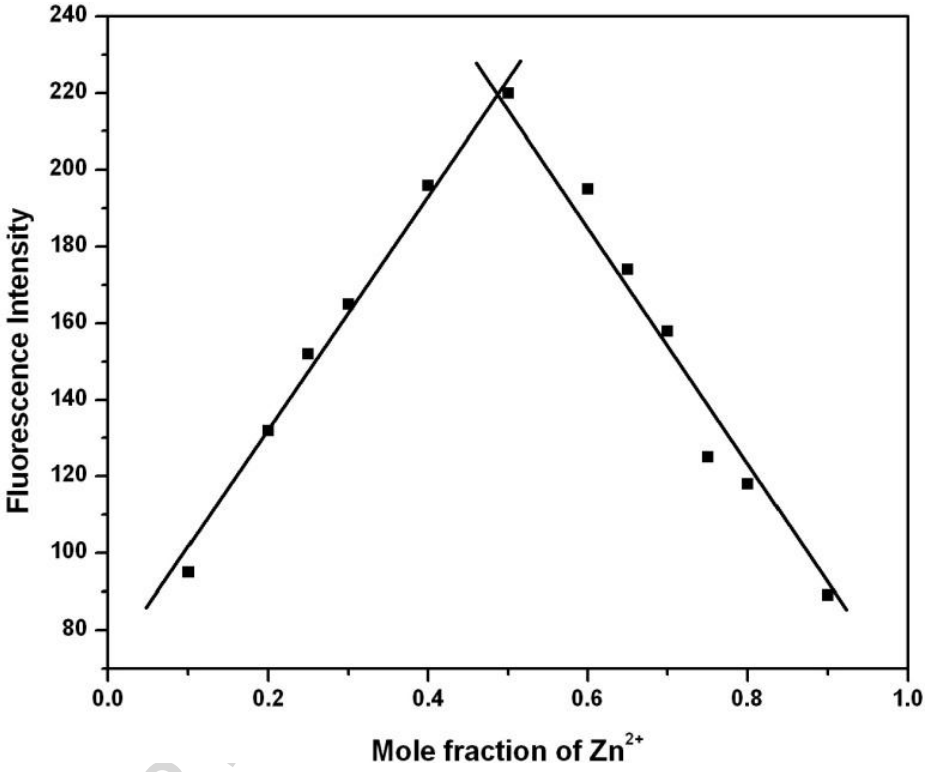

Fig 5. Job's plot for the complex formed between receptor PY and Zn^{2+}

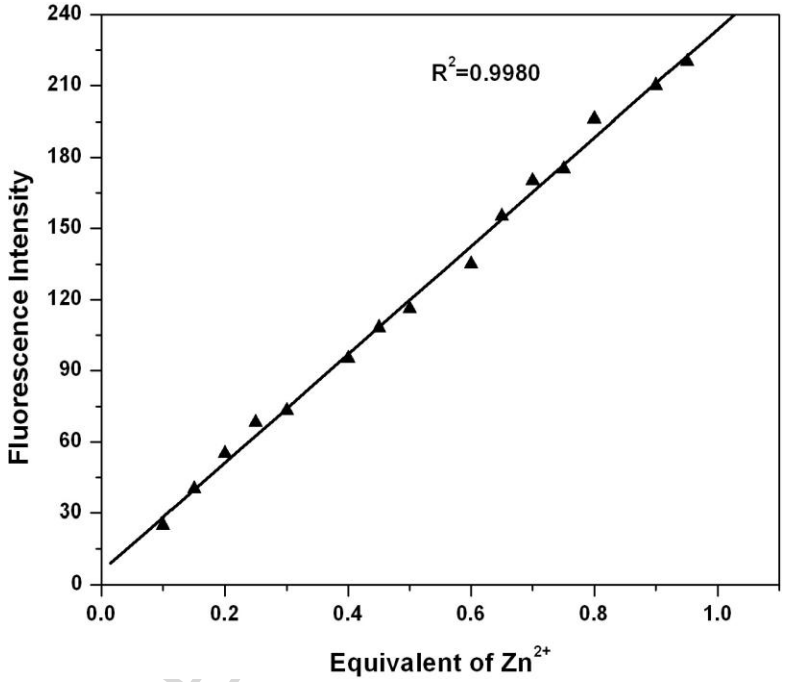

Fig 6. Plot of fluorescence intensity variation at 458nm upon varying equivalents of Zn^{2+} ions

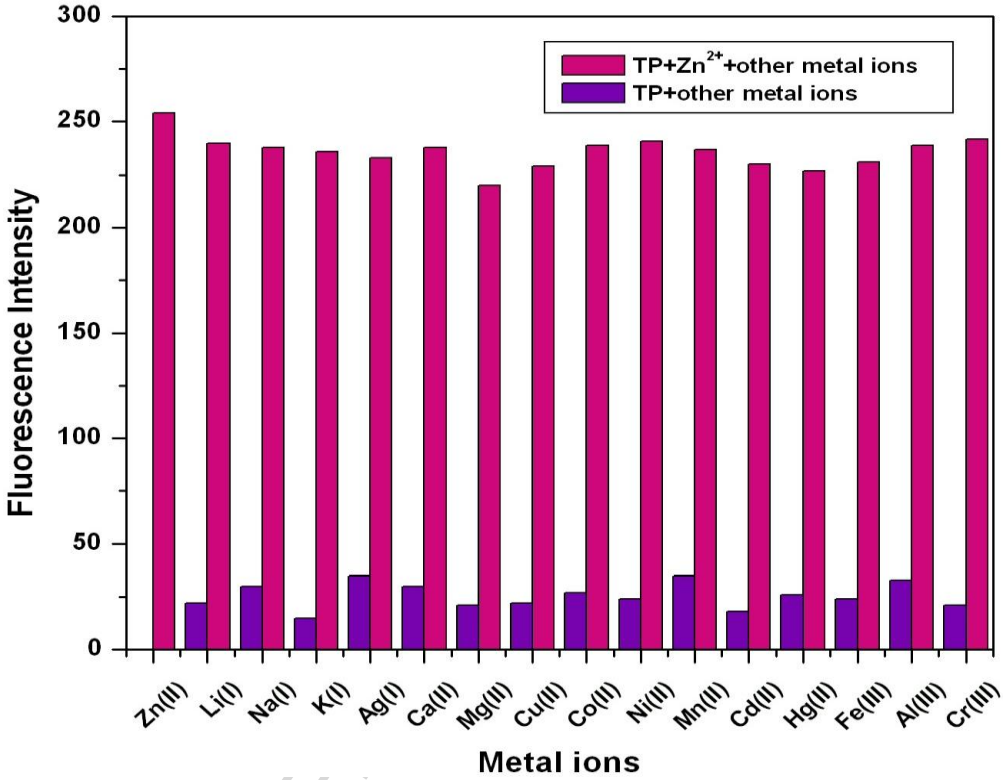

Fig 7. The fluorescence intensity of PY(10µM) in the presence of 20µM for Na^{+}, K^{+}, Li^{+}, Ag^{+}, Ca^{2+}, Mg^{2+}, Cu^{2+}, Co^{2+}, Ni^{2+}, Mn^{2+}, Zn^{2+}, Cd^{2+}, Hg^{2+}, Pb^{2+}, Cr^{3+}, Al^{3+}, Fe^{3+} (violet bars) followed by addition of 10µM of Zn^{2+} (pink bars) in aqueous DMSO[DMSO:H_2O=8:2] at pH = 7.4 (HEPES buffer).

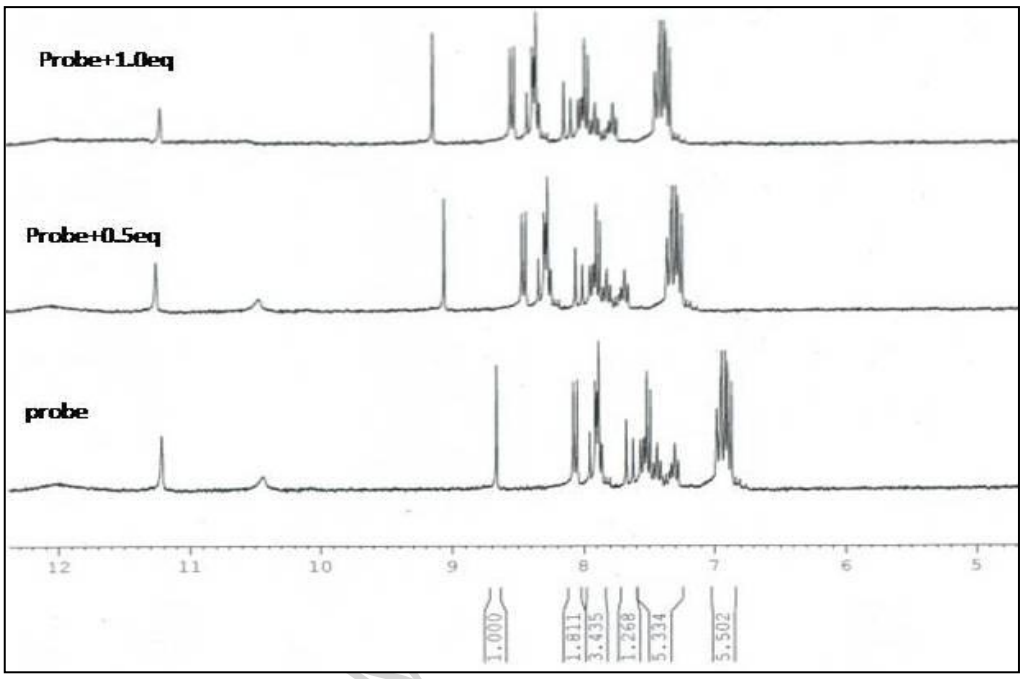

Excitation at 350nm (slit width=5nm)

Fig 8. Plot of ^{1}H NMR spectra of receptor PY(10µM) upon addition of Zn^{2+} in DMSO-d_6 at room tempertature

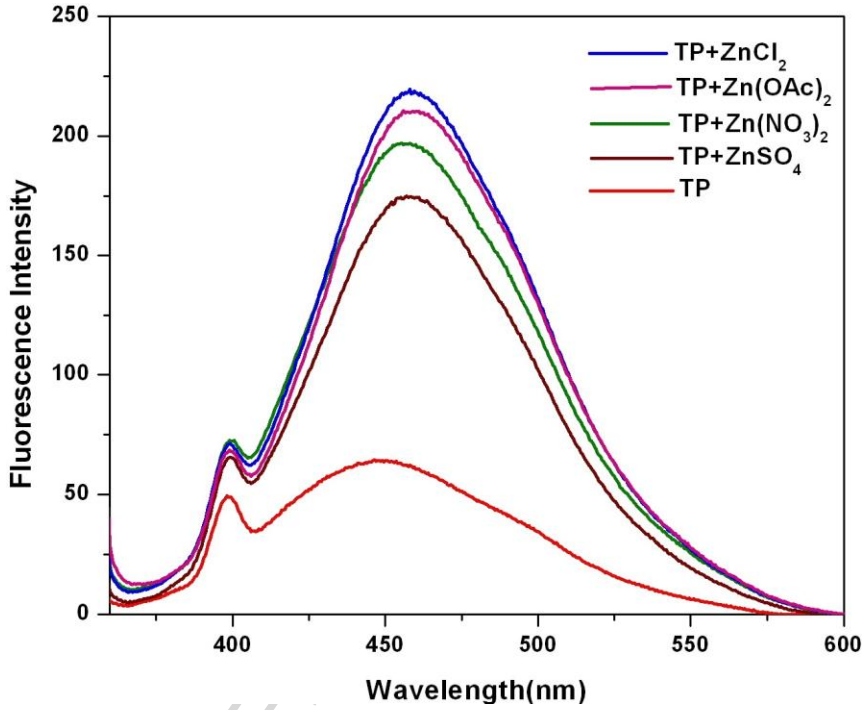

Fig 9. Fluorescent emission spectra of free receptor PY($1x10^{-5}$M) in aqueous DMSO[DMSO: H_2O=8:2] at pH = 7.4 (HEPES buffer) upon addition of 1.0 equivalent of different zinc salts

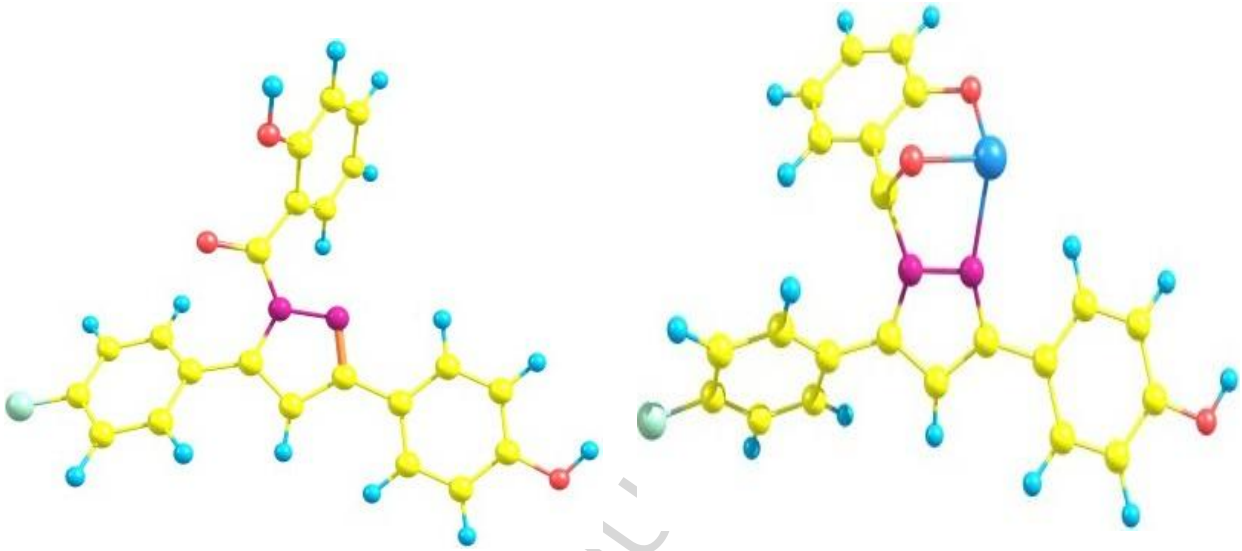

Fig 10. Conformations of PY(left) and PY.Zn^{2+}(right) optimized by density functional theory calculations

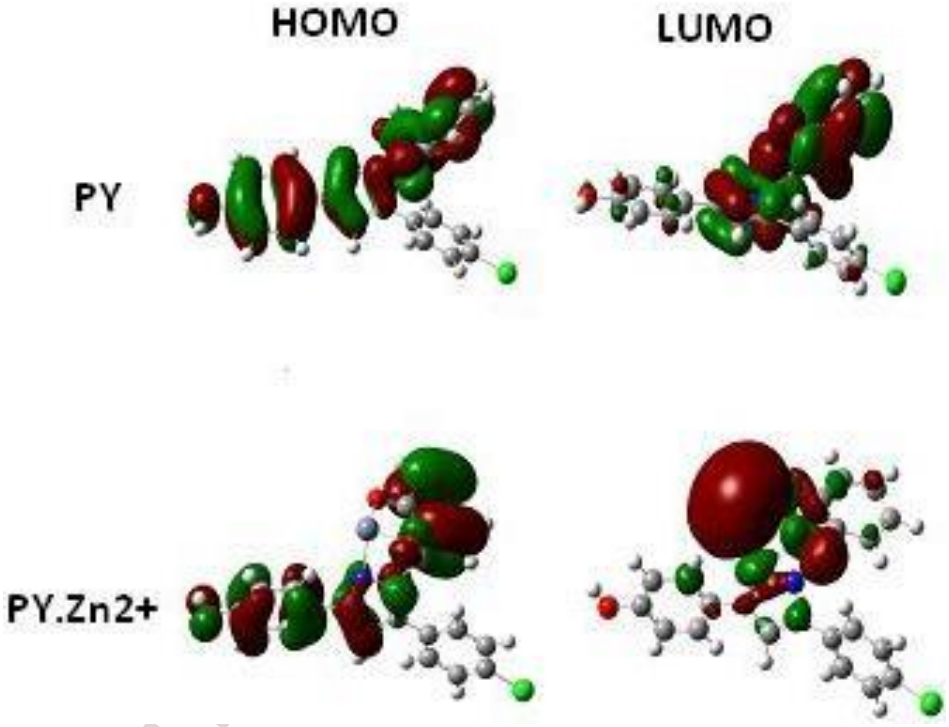

Fig 11. HOMO and LUMO plot of PY & PY/Zn^{2+} calculated at B3LYP/LANL2DZ(d) level of theory

Table 1: The binding constant comparison of our probe with sensors available in the literature

Probe	Binding constants	References
Receptor PY	$2.4x10^{4}M^{-1}$	Present study
Carboxamidoquinoline based macrocycle	$6.7x10^{6}M^{-1}$	1
Hydrazone-pyrene derivative	$2.4x10^{4}M^{-1}$	2
Tryptophan based Schiff base	$3.0x10^{4}M^{-1}$	3
Aminoacid based Schiff base	$1.1x10^{4}M^{-1}$	4
Pyrene derived molecule	$1.8x10^{6}M^{-1}$	5
Benzimidazole based receptor	$1.4x10^{4}M^{-1}$	6
Benzoimidazole dye	$7.4x10^{3}M^{-1}$	7

References

1. Y. Zhang, X. Guo, W. Si, L. Jia, X. Qian, Org. Lett., 10 (2008) 473-476.
2. Y. Zhou, H.N. Kim, J. Yoon, Bioorg. Med. Chem. Lett., 20 (2010) 125-128.

3. L. Li, Y.Q. Dang, H.W. Li, B. Wang, Y. Wu, Tetrahedron Lett., 51 (2010) 618-621.
4. L. Li, F. Liu, H.W. Li, Spectrochim. Acta A, Mol. Biomol. Spectrosc., 79 (2011) 1688-1692.
5. E. Manandhar, J.H. Broome, J. Myrick, W. Lagrone, P.J. Cragg, K.J. Wallace, Chem. Comm., 47 (2011) 8796-8798.
6. M.J. Kim, K. Kaur, N. Singh, D.O. Jang, Tetrahedron, 68 (2012) 5429-5433.
7. X. Wang, Z. Liu, F. Qian, W. He, Inorg. Chem. Comm., 15 (2012) 176-179.

Table 2: The detection limit comparison of our probe with sensors available in the literature

Probe	Detection limits	References
Receptor PY	1.02µM	Present study
Pyrazole	0.12µM	1
Napthyl imino conjugate	2.4µM	2
MCB dye	$2.5x10^{-8}$M	3
Self-assembled monolayer receptor	$1.7x10^{-5}$M	4
Napthaldehyde based Schiff base	$1.0x10^{-7}$M	5
Benzimidazole based receptor	3.0µM	6
Pyrazoline derivative	$6.1x10^{-7}$M	7

References

1. Z.L. Gong, F. Ge, B.X. Zhao, Sens. Actuators, B. 159 (2011) 148-153.

2. A. Mitra, V.K. Hinge, A. Mittal, S. Bhakta, P. Guionneau, C.P. Rao, Chem. Eur. J., 17 (2011) 8044-8047.
3. N. Aksuner, E. Henden, B. Yenigul, I. Yilmax, A. Cukurovali, Spectrochim. Acta A, Mol. Biomol. Spectrosc., 78 (2011) 1133-1138.
4. D.W. Kim, K.K. Kim, E.B. Lee, J.S. Kim, J. Photochem. Photobiol. A: Chem., 250 (2012) 33-39.
5. R. Azadbakht, H. Keypour, Spectrochim. Acta A, Mol. Biomol. Spectrosc., 85 (2012) 293-297.
6. M.J. Kim, K. Kaur, N. Singh, D.O. Jang, Tetrahedron, 68 (2012) 5429-5433.
7. Z. Zhang, F.W. Wang, S.Q. Wang, F. Ge, B.X. Zhao, J.Y. Miao, Org. Biomol. Chem., 10 (2012) 8640-8644.

Graphical abstract

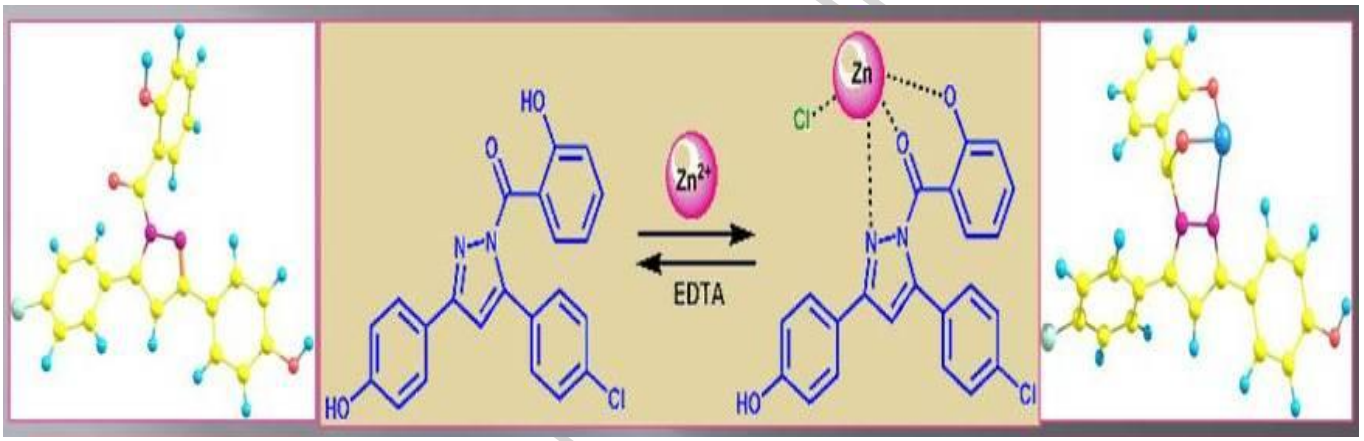

Highlights

- The receptor **PY** was synthesized by a simple method with high yield
- The detection limit of Zn^{2+} by **PY** was very low (1.02μM)
- The reversible behavior of the receptor **PY** towards Zn^{2+} was studied with EDTA
- The turn-on response with remarkable red shift in the fluorescence spectra was further supported by quantum(DFT) calculations